A self-powered, one-step chip for rapid, quantitative and multiplexed detection of proteins from pinpricks of whole blood†

Jun Wang,[abc] Habib Ahmad,[abc] Chao Ma,[abc] Qihui Shi,[abc] Ophir Vermesh,[abc] Udi Vermesh[abc] and James Heath*[abc]

Received 19th June 2010, Accepted 9th September 2010
DOI: 10.1039/c0lc00132e

We describe an automated, self-powered chip based on lateral flow immunoassay for rapid, quantitative, and multiplex protein detection from pinpricks of whole blood. The device incorporates on-chip purification of blood plasma by employing inertial forces to focus blood cells away from the assay surface, where plasma proteins are captured and detected on antibody "barcode" arrays. Power is supplied from the capillary action of a piece of adsorbent paper, and sequentially drives, over a 40 minute period, the four steps required to capture serum proteins and then develop a multiplex immunoassay. An 11 protein panel is assayed from whole blood, with high sensitivity and high reproducibility. This inexpensive, self-contained, and easy to operate chip provides a useful platform for point-of-care diagnoses, particularly in resource-limited settings.

Introduction

Blood contains the most complete version of the human proteome, and so provides a rich and convenient source of information for disease diagnostics.[1–3] Conventional clinical blood protein diagnostic measurements are quantitative, but also time-consuming. They require multiple steps, a significant amount of blood sample, and can be awkward to multiplex when assaying large panels of protein biomarkers, although there is recent progress in this area.[4–6] By contrast, lateral flow point-of-care (LF-POC) devices, which are widely used for rapid detection of blood biomarkers from patients in developing world settings, are inexpensive, self-contained, simple to operate, and usually require only small blood samples. However, they are neither quantitative nor multi-parameter.[7] Herein we report on a technology we call the Lateral Flow Integrated Blood Barcode Chip (LF-IBBC) that is designed to encapsulate many of the advantages of both standard and POC protein diagnostics while also providing highly multiplexed measurements. The LF-IBBC represents a significant advance over our previously reported blood protein assay chips[4,8] in terms of design simplicity, measurement accuracy and reproducibility, and ease of manufacture and use.

Fig. 1 shows a summary of several of the design and operational aspects of a LF-IBBC. The chip is comprised of a microfluidic layer fabricated from a hydrophilic polymer (NOA-63) that is bonded to a glass microscope slide. Prior to assembly, the microscope slide is patterned with DNA barcodes[4,9] (see Methods); thereafter, the LF-IBBC is stable towards long-term storage. For blood protein assays, the DNA barcodes are converted into antibody barcodes using the DNA-encoded antibody library technique (DEAL).[10–13] About 30 min (or less) prior to use, the fluidic chambers 1, 2, and 3 are filled with the appropriate reagents (see the labels on Fig. 1a). To operate the chip, a few microlitres (μl) of whole blood, with an anticoagulant, are added into chamber 4 (Fig. 1a), and a filter paper is inserted into the outlet slot shown at right. The capillarity of the filter paper, coupled with the hydrophilic nature of the fluidic channel surfaces, sequentially draws the blood and other reagents through the chip, with the blood drawn first, and the wash buffer drawn last (see labels of Fig. 1a). Thus, each step of a standard enzyme-linked immunosorbent assay (ELISA) is automatically and sequentially executed (Fig. 1d). The blood and reagents pass from the chambers through a narrow channel, before exiting into a wider assay channel. This scheme results in inertial focusing of the blood cells into a central stream within the assay channel (Fig. 1b) so that the assay surface is exposed only to flowing plasma. During the flow-through process, serum biomarker proteins are selectively captured onto specific stripes within the antibody barcodes (Fig. 1c). The blood protein levels are recorded in about 10 minutes after pinprick sampling, and the entire assay development process takes ~40 minutes. A GenePix array scanner is utilized to record the fluorescence levels from the individual barcode stripes, and automated software routines convert those levels into protein abundances. Each barcode constitutes a complete copy of the panel of blood biomarker proteins assayed, and multiple barcodes are measured and averaged per pinprick assay.[4]

Results and discussion

Plasma separation from whole blood

For POC lateral-flow devices, a single paper film can provide a filter for at least partially separating cells from whole blood, it

[a]*NanoSystems Biology Cancer Center, California Institute of Technology, MC 127-72, 1200 E. California Blvd., Pasadena, California, 91125, USA. E-mail: heath@caltech.edu; Tel: +1 626 395 8920*
[b]*Kavli Nanoscience Institute, California Institute of Technology, MC 127-72, 1200 E. California Blvd., Pasadena, California, 91125, USA*
[c]*Division of Chemistry and Chemical Engineering, California Institute of Technology, MC 127-72, 1200 E. California Blvd., Pasadena, California, 91125, USA*

† Electronic supplementary information (ESI) available: Figures S1–S7, Tables S1 and S2, Videos S1–S6, and Methods. See DOI: 10.1039/c0lc00132e

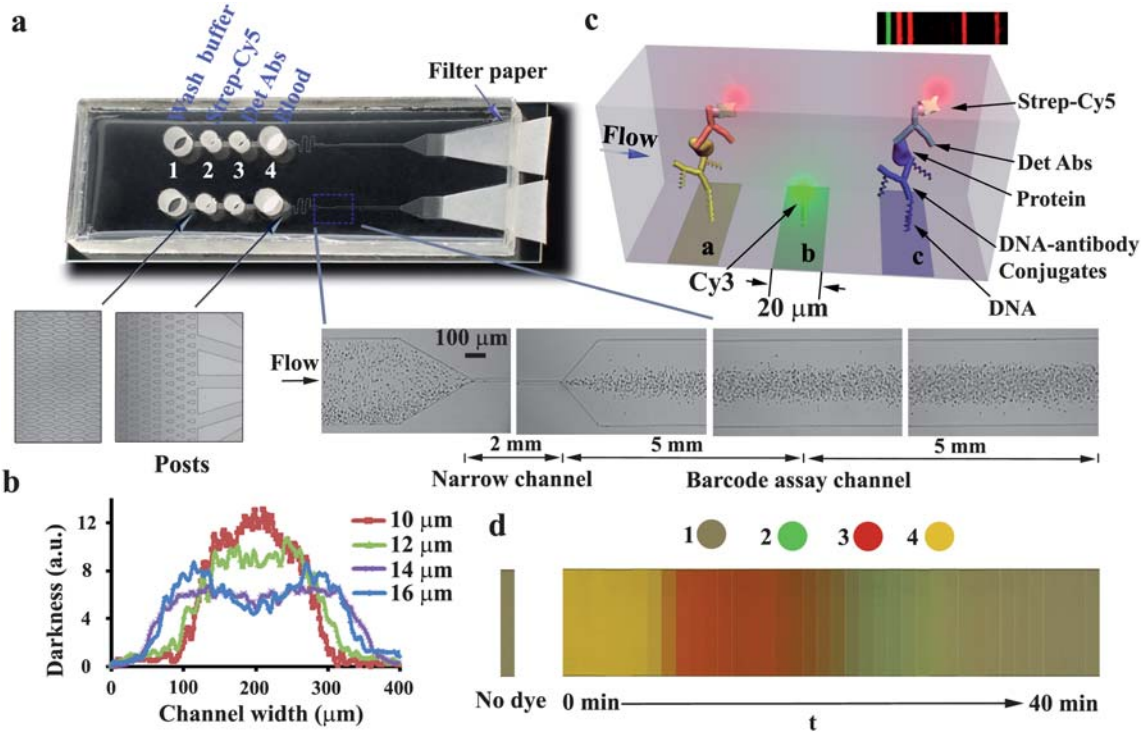

Fig. 1 LF-IBBC design and operation. (a) Photograph of a chip containing two independently operated LF-IBBCs. The four reservoirs at left hold the indicated blood or reagents for completing a multiplexed ELISA assay. The higher resolution images below highlight design details. The channel connecting the chambers contains a high-density of microfabricated posts to filter impurities. A serpentile channel between chamber 4 and the narrow section provides for reagent mixing upstream of the assay region. Adsorbent paper inserted into a slot in the waste outlet sustains fluidic flow due to capillary action. Inertial focusing spatially separates plasma from whole blood, keeping the assay surface clear of blood cells over the length of the barcode assay channel. (b) Plot showing how the diameter of the focusing channel influences the width of the fluid centroid that contains the blood cells. (c) Proteins are detected using a variant of standard ELISA assays in which a barcode pattern of DNA-labeled capture antibodies provides a spatial address for each protein in the panel. The inset represents a fluorescent readout of a completed barcode assay. (d) Real-time colorimetric imaging of a solution flowing through a section of the barcode assay channel. Chambers 4, 3, 2, and 1 were loaded with 10, 8, 8, and 10 μl of dye solutions, respectively (see color code). The evolving colors illustrate the time scale for the filter paper to sequentially drain the channels and complete the assay.

can provide capillarity for pulling the blood and assay reagents through the platform, and it can provide the assay surface (*i.e.* an antibody-coated region of the paper is colorized if a certain biomarker is present in the blood). We borrow some of these concepts here. First, a small paper pre-filter is inserted into the base of the blood chamber (chamber #4), which serves to remove 80–90% of the cells from the blood. This pre-purification, along with the filter posts patterned into the microfluidic channel in the region near the inlet chambers, keeps the chip from clogging, but is insufficient for a quantitative and sensitive protein assay. Further purification is achieved by pulling the blood through a 10–20 μm wide, 2 mm long narrow channel (Fig. 1a and S1, ESI†), before it exits into the much wider (500 μm wide), 1.5 cm long barcode assay channel. Inertial lift forces were employed to axially focus the cells within the assay channel. Such forces have been well-studied, and have multiple contributions that include the wall-effect force and the shear-lift force.[14–17] The wall-effect force, for example, describes forces that are normal to a wall, and are experienced by a particle that is flowing parallel to that wall. This force thus pushes particles towards the center-line. The net result is that the blood cells do not interfere with the protein assays. Fig. 1b illustrates how the dimensions of the narrow channel influence the column diameter of the focused blood cells. The final design dimensions of the narrow channel (2 mm long, 12 μm wide) provided excellent focusing along the entire length of the assay channel for both spherical cells and disk like erythrocytes (Fig. 1b and S2, ESI†), thus keeping the assay surface clear of blood cells. In general, the extent of focusing also depends upon the flow rate (Videos 1–5,ESI†), although for the current design this dependence is weak (Fig. S2, ESI†). This design thus permits a seamless integration of a plasma separation function with a lateral-flow immunoassay, all within the same microfluidic channel, and without skimming, and so takes advantage of a larger fraction of the plasma than a Zweifach–Fung design.[18–20]

Powering fluidic flow

The high-wettability filter paper inserted at the waste outlet of the chip draws flow for >2 h. Reliable fluid flow also requires hydrophilic microchannel surfaces. Although the commonly used microfluidic elastomer, polymethylmethacrylate (PMMA), can be made hydrophilic by O_2 plasma treatment, use of the naturally hydrophilic polymer NOA 63 yielded a more stable and robust solution. We calibrated the filter-paper driven flow through an LF-IBBC using a mass-flow controlled syringe-pump

powered chip. Using measurements of the trajectory of flowing cells (driven by the two different power sources) we were able to estimate that the filter paper pulls solutions at a velocity of 0.67–1.34 mm s^{-1} (0.5–1 μl min^{-1}) through the barcode assay channel (Videos S2, S3 and S5, ESI†). Reagent chambers are drained sequentially, so that the blood in chamber #4 is depleted first, followed by chambers 3, 2, and 1. The dense posts between the reagent chambers are designed to filter impurities as well as increase flow resistance. This potentially retards mixing of fluids in one chamber with those from the neighboring chambers during stepwise depletion. In addition, the capillarity in each chamber can also contribute to the stepwise depletion since typically as the fluid within a chamber is drained, the relative meniscus height increases. We recorded the stepwise depletion effect by loading different dyes into the four chambers, and then imaging the fluid, over time, at a fixed point in the barcode assay channel (Fig. 1d and Video S6, ESI†). Each color dominated the image for about 10 min. Thus, each of the steps constituting a standard ELISA assay, from sample introduction to secondary antibody binding, fluorophore binding, and washing, are executed without human intervention (Fig. S4b, ESI†).

Multiplex protein barcode assay

The microfluidic-based flow patterning technique generates DNA barcode-type arrays, comprised of 20 μm wide stripes at a 50 μm pitch, that are 10× higher density than standard, spotted microarrays.[4] The barcodes are patterned over the majority of the glass slide surface, which alleviates the need for alignment of the LF-IBBC assay channel with the barcodes during chip assembly. The DNA barcodes are stable against both the subsequent microfluidics fabrication steps and long term chip storage. They are converted into antibody barcodes by flowing through a cocktail of DNA-labeled antibodies against the proteins within the biomarker panel. Each antibody is labeled with ~3 copies of a ssDNA oligomer that is complementary to one of the ssDNA barcode stripes, but orthogonal to all other stripes. Sequences of the DNA oligomers used here are given in Table S1, ESI†, and the antibody pairs used are presented in Table S2, ESI†.

The DNA flow patterning procedure generates DNA barcode stripes of very high aspect ratio: 20 μm width and ~0.5 m long. We optimized the flow-patterning technique to emphasize high and uniform DNA loading over the entire length of the stripes (see Methods). We previously demonstrated that these improved barcodes could be utilized to assay a panel of cytoplasmic proteins from a single lysed cancer cell.[9] Here we demonstrate the use of those barcodes for detecting a panel of blood proteins using the LF-IBBC. We assayed freshly collected pinpricks of blood for a panel of 11 proteins. These proteins were *C*-terminal reactive protein (CRP), matrix metalloproteinase 3 (MMP3), serine proteinase inhibitor (Serpin), granulocyte colony-stimulating factor (GCSF), macrophage migration inhibitor factor (MIF), epidermal growth factor (EGF), chemokine (C–C motif) ligand 5 (CCL5), vascular endothelial growth factor (VEGF), interleukin 8 (IL-8), IL-1β, and interferon-γ-induced protein (IP 10). These proteins are variously associated with tumor progression, inflammation, and other disease conditions.[21–24] Stripe 12 was functionalized with mouse IgG1 isotype control to measure the level of non-specific binding for the assay. Quantitation and assay cross-reactivity data for this panel are provided in Fig. S5, ESI†.

In Fig. 2 we present data collected from assaying the biomarker panel from a pinprick of whole blood on a LF-IBBC. A contact-activated lancet was employed to prick a finger of a healthy donor. Immediately thereafter, a capillary blood collection tube prefilled with 1 μl of 150 mM citrate anticoagulant solution was used to collect ~10 μl blood, which was then transferred to chamber #4 of 3 separate LF-IBBC (for triplicate measurements to test the reproducibility of the barcode assays) with chambers 1–3 already pre-filled with their designated reagents. Filter paper was inserted at the end of the device, and after 40 minutes the assay was complete. The microfluidic layer was peeled off the glass slide, and the barcode fluorescence intensities were scanned and digitized using a GenePix array scanner and custom written software. In Fig. 2a we present eight barcode assays, both in image and digitized form, from one of these chips. These assays, along with the statistical analysis of Fig. 2b, illustrate how highly uniform barcoding chemistry translates into highly reproducible protein assays. Four of the proteins in the panel, including VEGF (detection limit ~60 pg ml^{-1} (1.3 pM)) and IL-8 (detection limit ~20 pg ml^{-1} (2.5 pM)), were below the detection threshold, which is not surprising for a healthy donor. The detection limits for the LF-IBBC assays are only slightly higher than the manufacturer specifications for the individual ELISA assays (~15 pg ml^{-1} for IL8 and ~30 pg ml^{-1} for VEGF).

At sufficiently high flow velocity, the time to complete a flow-through assay is limited by the kinetics of antibody/analyte binding,[25] rather than by diffusion (as in a standard 96-well plate format). The flow velocity of blood through the LF-IBBC barcode assay channel is ~1 mm s^{-1}, which implies that the LF-IBBC assay should be nearly kinetically limited, with each assay step requiring ~5 to 10 minutes. By varying the amount of fluids loaded in chambers 1–4, we varied the assay time (Fig. 3) and found that the amount of protein detected slightly increases between the 20 and 40 minute assays (corresponding to 5 and 10 min per step).

Conclusion

The Lateral-flow Integrated Blood Barcode Chip draws from advantages presented by standard, quantitative blood immunoassay procedures and point-of-care lateral flow immunoassays. Whole blood is readily handled on-chip *via* a hydrodynamic focusing scheme that spatially separates cells and plasma within the same fluidic channel. Adsorbent filter paper provides power to drive all the steps of a quantitative, highly multiplexed ELISA-like immunoassay. In addition, a reproducible patterning technology for preparing antibody barcodes integrated into the microfluidic assay channels provides for both a high level of sensitivity and quantitation for rapidly assessing the levels of a panel of blood proteins.

Materials and methods

Microchip fabrication

General procedures for microchip fabrication using polydimethylsiloxane (PDMS) were described previously.[26] A high-resolution chrome mask was used for photolithography; its features were replicated on a 4 inch silicon wafer with negative

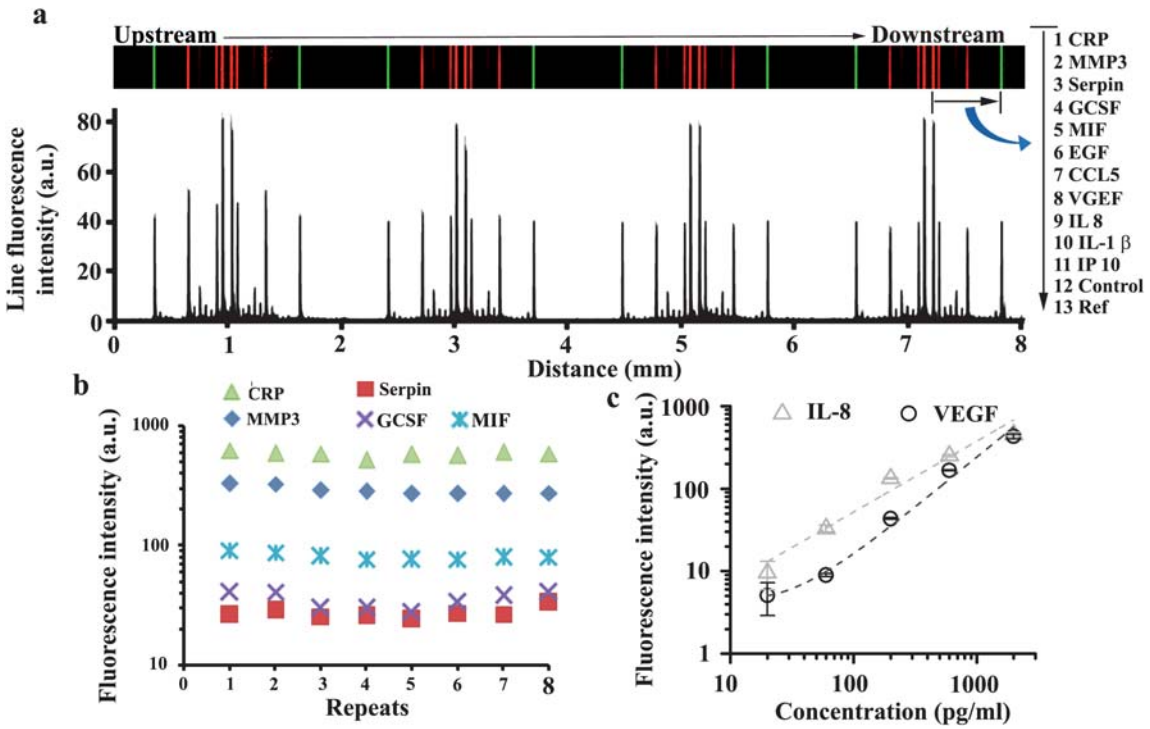

Fig. 2 Multiplex LF-IBBC protein assay from whole blood. (a) A representative fluorescence image of 8 barcodes each recording an identical panel of 11 proteins. Each barcode is bounded by a green fluorescent alignment marker. Each red bar records a unique protein; protein locations are determined relative to the alignment markers. The integrated fluorescence intensity of the 8 barcodes is presented below the fluorescent image, and reflects how reproducible barcode patterning leads to reproducible protein assays. (b) Fluorescence intensity of the first 5 biomarkers at each barcode repeat. (c) Correlation of the fluorescence intensity and corresponding protein concentrations for IL-8 and VEGF in logarithmic scale. The data reflect a better than 10% measurement error, except for the proteins present at the lower detection limits (<20 pg ml^{-1}). Eight whole barcodes were used to generate the mean fluorescence intensities and measurement uncertainties. The dashed lines are power law fits to guide the eyes.

photoresist (SU-8 2025, Microchem), yielding a master for molding PDMS (Methods, ESI†). Masters for fabricating NOA 63 (Norland) devices required further treatment: a layer of aminosilane was grafted on the surface of the master mold by O_2 plasma activation at 25 W for 30 s, followed by immersion in 2% 3-(aminopropyltriethoxysilane) (APTES, Sigma-Aldrich) in acetone for 10 min. The master was washed sequentially with isopropanol and DI water before an N_2 blow dry. A thin layer of monoglycidyl ether-terminated PDMS (Sigma-Aldrich) was spun with a speed of 1000 rpm for 30 s on the modified master, and subsequently incubated at 80 °C for 4 h. The master was then cleaned with isopropanol and dried under streaming N_2. The resulting PDMS monolayer on the master prevented NOA 63 from sticking to the surface.[27] To make a NOA replica, an aluminium plate with cutouts was fitted over the silicon master such that the SU-8 features were exposed through the cutouts. NOA 63 was poured into the cutouts, and the assembly was treated for 5 minutes with UV exposure before the NOA replica was peeled off. The replica was further processed by drilling chamber holes with a standard drill press and trimmed to appropriate dimensions. Finally, UV treatment was performed again to render the surface permanently hydrophilic before bonding to a DNA-patterned barcode array slide.[27,28]

Barcode array patterning

The high-density DNA microarray was patterned using a microfluidic device also fabricated by soft-lithography (Fig. S3, ESI†). In order to generate highly consistent barcode arrays, a silicon hard master was generated by transferring photolithographically defined patterns into an underlying silicon wafer using deep reactive ion etching (DRIE). Following standard soft-lithography procedures, a pre-cure PDMS mixture was poured onto the hard master and heated at 80 °C for 40 min. The PDMS replica was cutout, access holes to the channels were punched, and the device was bonded to a polylysine glass slide (Erie Scientific Company) at 80 °C for 1 hour. The barcode device consists of 20 microchannels, each 20 μm wide and spaced at a 30 μm interval, winding across a 1.5″ × 1″ area. Thirteen of those channels were individually filled with unique 30–33mer oligonucleotides A–M (sequences in Table S1, ESI†), each at a concentration of 266 μM in 33% DMSO; a simple 3 psi pressure gradient was used to drive flow. The DNA solutions were allowed to evaporate in a desiccator, after which the PDMS device was removed and the glass substrate was baked at 80 °C for 4 h. Finally, the substrate was thoroughly washed with DI water to yield a barcode array slide that could be stored under desiccation for months.

Collecting finger-prick blood

The collection procedure complies with the protocol approved by the Institutional Review Board of the California Institute of Technology. A microtainer contact-activated lancet (BD Science) was used to obtain ~10 μl of blood from a healthy

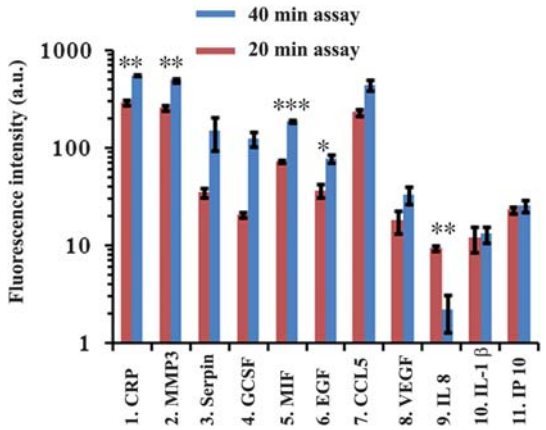

Fig. 3 Statistical comparison of 20 min and 40 min multiplexed protein assays using a LF-IBBC and pinpricks of whole blood from a single healthy donor. Mean fluorescence intensities are presented for each biomarker. Each measurement was performed in triplicate using 3 separate LF-IBBCs, but the same pinprick sample from a healthy donor. For each individual LF-IBBC assay, 8 barcodes were averaged to yield the measured protein levels. For this bar graph, the 3 separate LF-IBBC assays were then averaged. The error bars represent the measured standard deviation across the three separate LF-IBBC measurements. Differences between the 20 and 40 min LF-IBBC assays are calculated using the two-tailed Student's *t*-test: (*), (**) and (***) indicate significant differences at $P < 0.05$, 0.01 and 0.001, respectively. The 40 min assay is clearly the most sensitive, but increasing assay times an additional 25–30% did not further increase sensitivity.

donor. The whole blood was collected with SAFE-T-FILL capillary blood collection tubes (RAM Scientific) which are prefilled with 1 μl of 150 mM citrate solution as an anti-coagulant, and then immediately transferred to the one-step chip for analysis. Any surface contaminated by blood was disposed of according to standard biohazard disposal protocols.

Blood cell self-focusing observation

The narrow focusing section was fabricated at various lateral dimensions while maintaining an identical 31 μm height. A syringe pump was used to generate steady flow rates for blood through the microchannels, and visual comparison of blood cell flow powered by filter paper and syringe pumps led to estimated flow rates in the barcode readout channel. Cell focusing profiles were generated by superimposing 50 consecutive images taken at the middle of the barcode readout channel with exposure time 0.187 s, and subsequently inverting the white/black color.

Microchip operation and observation

The capture antibody array was created using the DEAL technique (Fig. S4 and Methods, ESI†). Prior to loading any solutions, a piece of asymmetric polysulfone membrane (PALL) was placed at the bottom of the blood chamber 4 (Fig. 1). A piece of filter paper (grade 50, Whatman) was placed at the end of the microchannel. The blocking step was performed by adding 20 μl 3% w/v bovine serum album (BSA, Sigma-Aldrich) in phosphate buffer saline (PBS) to chamber 4. Induced by capillary flow, the BSA solution spontaneously filled up all channels within 5 min. After 20 min, the chambers were drained by pipetting to remove residual solutions. Chamber 4 was refilled with 10 μl of a cocktail containing 11 DNA-labeled antibodies (Table S2, ESI†), at a concentration of 25 μg ml^{-1}. Chamber 3 was filled with 10 μl 3% BSA (Fig. S4a, ESI†). The microchip was ready to run when all the chambers were depleted of solutions. Alternatively, the chip may be sealed and stored in a refrigerator at 4 °C after removal of the filter paper. No obvious alteration of the DEAL antibody array quality was observed after one month of storage (data not shown).

To perform a 40 min assay, 7 μl of whole blood sample, 5 μl detection antibodies (Det Abs) at 25 μg ml^{-1}, 5 μl streptavidin–cy5 at 10 μg ml^{-1} and 15 μl 3% BSA w/v in PBS were loaded into chambers 4, 3, 2, and 1, respectively (Fig. S4b, ESI†). To test assay sensitivity, a 7 μl aliquot of a solution of recombinant proteins at designated concentrations in 1% BSA/PBS solution replaced the blood sample. 20 min assays were conducted by halving the amount of reagents in each chamber. All assays were conducted at room temperature, although ongoing study found that sensitivity tended to be higher as environmental temperature rose.

Data analysis and statistics

The LF-IBBC can be read directly under a fluorescence microscope. However, we adopted a GenePix 2000B (Axon Instruments) array scanner for data acquisition, since it is designed for similar purposes for spotted arrays. Before GenePix analysis, the glass substrate was separated from the elastomer chip and immediately dipped 3 times in freshly prepared PBS solution with 0.05% Tween 20, followed by 2 dips in DI water and air drying. The GenePix scanner contains dual lasers with appropriate optical filters to detect Cy3 at 532 nm and Cy5 at 635 nm. The parameters for the scanner were set as follows: laser power 80% and gain 600 for Cy5, laser power 15% and gain 450 for Cy3. The fluorescence signal profile was processed by ImageJ (NIH) and a custom-written Excel macro. The fluorescence intensity of barcodes in each device was extracted and averaged. The standard deviations of those barcodes represent error bars, which indicate self-consistency of assay. To assess the effect of assay time, the mean fluorescence intensity of barcodes from each assay time (triple repeats) was obtained and Student's *t*-test was applied to calculate *P*-value at a significance level of at least 0.05.

Acknowledgements

This work was supported by the National Cancer Institute Grant No. 5U54 CA119347 (J.R.H. and P.I.), by a gift from the Jean Perkins Foundation and by the Ben & Catherine Ivy Foundation.

References

1 N. L. Anderson and N. G. Anderson, *Mol. Cell. Proteomics*, 2002, **1**, 845–867.
2 S. Ray, M. Britschgi, C. Herbert, Y. Takeda-Uchimura, A. Boxer, K. Blennow, L. F. Friedman, D. R. Galasko, M. Jutel, A. Karydas, J. A. Kaye, J. Leszek, B. L. Miller, L. Minthon, J. F. Quinn, G. D. Rabinovici, W. H. Robinson, M. N. Sabbagh, Y. T. So, D. L. Sparks, M. Tabaton, J. Tinklenberg, J. A. Yesavage,

R. Tibshirani and T. Wyss-Coray, *Nat. Med. (N. Y., NY, U. S.)*, 2007, **13**, 1359–1362.
3 A. A. Kamat, M. Baldwin, D. Urbauer, D. Dang, L. Y. Han, A. Godwin, B. Y. Karlan, J. L. Simpson, D. M. Gershenson, R. L. Coleman, F. Z. Bischoff and A. K. Sood, *Cancer*, 2010, **116**, 1918–1925.
4 R. Fan, O. Vermesh, A. Srivastava, B. K. H. Yen, L. D. Qin, H. Ahmad, G. A. Kwong, C. C. Liu, J. Gould, L. Hood and J. R. Heath, *Nat. Biotechnol.*, 2008, **26**, 1373–1378.
5 L. Gervais and E. Delamarche, *Lab Chip*, 2009, **9**, 3330–3337.
6 A. W. Martinez, S. T. Phillips, M. J. Butte and G. M. Whitesides, *Angew. Chem., Int. Ed.*, 2007, **46**, 1318–1320.
7 G. A. Posthuma-Trumpie, J. Korf and A. van Amerongen, *Anal. Bioanal. Chem.*, 2009, **393**, 569–582.
8 L. D. Qin, O. Vermesh, Q. H. Shi and J. R. Heath, *Lab Chip*, 2009, **9**, 2016–2020.
9 Y. S. Shin, H. Ahmad, H. J. Kim, Q. H. Shi, T. A. Charles-Pascal, R. Fan, W. A. Goddard and J. R. Heath, *ChemPhysChem*, 2010, DOI: 10.1002/cphc.201000528.
10 G. F. Zheng, F. Patolsky, Y. Cui, W. U. Wang and C. M. Lieber, *Nat. Biotechnol.*, 2005, **23**, 1294–1301.
11 R. C. Bailey, G. A. Kwong, C. G. Radu, O. N. Witte and J. R. Heath, *J. Am. Chem. Soc.*, 2007, **129**, 1959–1967.
12 C. Boozer, J. Ladd, S. F. Chen and S. T. Jiang, *Anal. Chem.*, 2006, **78**, 1515–1519.
13 C. M. Niemeyer, *Nano Today*, 2007, **2**, 42–52.
14 P. Cherukat and J. B. Mclaughlin, *J. Fluid Mech.*, 1994, **263**, 1–18.
15 M. Yamada, M. Nakashima and M. Seki, *Anal. Chem.*, 2004, **76**, 5465–5471.
16 S. C. Hur, H. T. K. Tse and D. Di Carlo, *Lab Chip*, 2010, **10**, 274–280.
17 J. Wang, Y. H. Zhan, V. M. Ugaz and C. Lu, *Lab Chip*, 2010, **10**, 2057–2061.
18 K. Svanes and B. W. Zweifach, *Microvasc. Res.*, 1968, **1**, 210–220.
19 Y. C. Fung, *Microvasc. Res.*, 1973, **5**, 34–48.
20 S. Yang, A. Undar and J. D. Zahn, *Lab Chip*, 2006, **6**, 871–880.
21 C. F. Nathan, T. J. Prendergast, M. E. Wiebe, E. R. Stanley, E. Platzer, H. G. Remold, K. Welte, B. Y. Rubin and H. W. Murray, *J. Exp. Med.*, 1984, **160**, 600–605.
22 A. D. Luster, *N. Engl. J. Med.*, 1998, **338**, 436–445.
23 B. Kaur, F. W. Khwaja, E. A. Severson, S. L. Matheny, D. J. Brat and E. G. Van Meir, *Neuro-Oncology (Durham, NC, U. S.)*, 2005, **7**, 134–153.
24 Y. S. Hamirani, S. Pandey, J. J. Rivera, C. Ndumele, M. J. Budoff, R. S. Blumenthal and K. Nasir, *Atherosclerosis*, 2008, **201**, 1–7.
25 M. Zimmermann, E. Delamarche, M. Wolf and P. Hunziker, *Biomed. Microdevices*, 2005, **7**, 99–110.
26 J. Wang, N. Bao, L. L. Paris, H. Y. Wang, R. L. Geahlen and C. Lu, *Anal. Chem.*, 2008, **80**, 1087–1093.
27 S. H. Kim, Y. Yang, M. Kim, S. W. Nam, K. M. Lee, N. Y. Lee, Y. S. Kim and S. Park, *Adv. Funct. Mater.*, 2007, **17**, 3493–3498.
28 E. P. Dupont, R. Luisier and M. A. M. Gijs, *Microelectron. Eng.*, 2010, **87**, 1253–1255.

